Paper ID APEN-MIT-2019_xxx
Applied Energy Symposium: MIT A+B
May 22-24, 2019 • Boston, USA

Assessing the Effect of Polyelectrolyte Complex Nanoparticles on Foam Film Stabilization and Oil Recovery in Carbonate Reservoir: An Environmentally Friendly EOR Method for Greenhouse Gas Management

Negar Nazari
Energy resources engineering department
Stanford University
Stanford, CA, USA
negar.nazari@stanford.edu

Hooman Hosseini
Chemical and petroleum engineering department
University of Kansas
Lawrence, KS, USA
h.hosseini@ku.edu

Jyun Syung Tsau
Tertiary Oil Recovery Program
University of Kansas
Lawrence, KS, USA
tsau@ku.edu

Karen Shafer-Peltier
Tertiary Oil Recovery Program
University of Kansas
Lawrence, KS, USA
kpeltier@ku.edu

Craig Marshall
Departments of Geology & Chemistry
University of Kansas
Lawrence, KS, USA
cpmarshall@ku.edu

Qiang Ye
Institute for Bioengineering Research
University of Kansas
Lawrence, KS, USA
yeq@ku.edu

Reza Barati Ghahfarokhi
Chemical and petroleum engineering department
University of Kansas
Lawrence, KS, USA
reza.barati@ku.edu

Abstract—Although CO_2 foam flooding is a proven technology to improve oil recovery; it has been criticized for lack of long term stability in saline environment and in the presence of crude oil. To generate a more stable foam front in the presence of crude oil and to overcome the capillary forces destabilizing the foam lamella, polyelectrolyte complex nanoparticles (PECNP) conjugated with surfactant oligomers were introduced to the lamella generated by high salinity aqueous phase to improve the EOR performance and produced water compatibility of supercritical CO_2 ($scCO_2$) foams. The formation of vesicular structures containing electrostatically hinged complexes of PECNP and surfactant was verified via transmission electron microscopy (TEM) while the structural changes associated with molecular complexation were identified using Raman spectroscopy. Accordingly, optimized ratios of PECNP: surfactant were employed to generate the most stable $scCO_2$ foam in high salinity produced water and to improve the recovery of the foam flooding process. Conducting core-flooding experiments in wide range of salinities indicated that the highest incremental oil recovery and the lowest residual oil saturation were achieved by prioritizing PECNP: surfactant $scCO_2$ foam flood.

Keywords: enhanced oil recovery, nanoparticles, foam film stability, produced water, CO_2 storage.

I. INTRODUCTION

Hydrocarbon resources are still the largest energy source on planet and account for approximately 67% of fossil energy [1]. To reduce detrimental environmental impacts of anthropogenic CO_2 emissions caused by usage of coal and hydrocarbon, compression, injection and partial storage in geological formations with the purpose of enhanced oil recovery (EOR) are viable approaches in oil recovery from subsurface resources [1].

CO_2 sequestration via EOR is a promising technique to reduce the greenhouse gas emission. Supercritical CO_2 is a potential candidate for CO_2 storage with properties such as improved mass transfer and increased selectivity [3]. Bernard and Holm introduced CO_2 foam as an effective mobility control agent with selective mobility reduction, to improve the sweep efficiency of EOR processes [2]. Aqueous based $scCO_2$ foam is a colloidal dispersion consisting of $scCO_2$ in water or brine and foaming stabilizers [4]. Contributing fluids give rise to the final viscosity of foam [4], eliminate pore plugging in the formation, and lower water-usage in water sensitive formations [3]. Large volumes of produced water from oil fields raises significant environmental concerns. Disposal, treatment and reuse are suggested options to handle produced water. Among them reinjection of produced water into the reservoirs is the most optimized and ecofriendly approach to handle the produced water [5].

The surfactant generated CO_2 foam stability in the presence of crude oil is a determining factor in oil recovery [5] and ultimately underground CO_2 storage [1]. Addition of polyelectrolytes with electrostatic conjugation to the surfactant solutions is considered a promising technique to improve foam film stability [6]. Nazari et al. [7] demonstrated that addition of polyelectrolyte and PECNP to the system, improves the foam stability and durability even in high salinity water in the presence or absence of crude oil.

In this work, the possibility of PECNP complexation with non-ionic surfactants capable of hydration for $scCO_2$ foams compatible with high salinity brines in CO_2-EOR is explored. The underlying mechanism for interaction of

PECNP: surfactant system with CO_2-high salinity brine interface during $scCO_2$ foam injection in underground formations is explored using multiple techniques including Raman spectroscopy, transmission electron microscopy (TEM), interfacial tension analysis, and core flooding experiments.

II. MATERIALS AND METHODS

A. Material synthesis and preparation

Synthetic brine was prepared in Reverse Osmosis (RO)-Deionized (DI) water according to a formulation from the Mississippian Limestone Play (MLP) produced water. The total dissolved solid in the brine was 235782.11 mg/L. Two salinities of 33,667 and 67,333 ppm were prepared by 6 and 3-times dilution of synthetic brine using RO-DI water, respectively.

The SURFONIC N-120 used in this study has 12 Ethylene oxide (EO) groups and it is provided by Huntsman Chemicals, Woodlands, TX, USA (CAS # 9016-45-9). The final surfactant concentration in all solutions was kept at 0.1 wt.% in both salinities to preserve the surface activity of the surfactant and to avoid the foam film stratification [7]. Branched PEI was purchased from Sigma Aldrich, St. Louis, MO, USA (CAS# 9002-98-6). The pH of PEI solutions was lowered to 8 by addition of 5.5 mL of 12 N Hydrochloric acid (HCl) to 600 mL of the PEI solution in both salinities. Dextran sulfate sodium salt (DS) is a polyanion in powder form and it was purchased from Fisher Chemical, St. Louis, MO, USA (CAS# 9011-18-1). The 1 wt.% PEI and DS solutions were prepared in both 33,667 and 67,333 ppm salinity brines.

To prepare the PECNP systems, the most optimized ratio of PEI: DS (3:1:0.1) was selected for both salinities based on the zeta potential and particle size measurements [7]. Subsequently, two ratios of 1:9 and 2:8 were selected for PEI: surfactant and the PECNP: surfactant solution ratios based on the foam durability analysis [7].

Mississippian crude oil, used for core-flooding experiments, has the asphaltenes content of 0.5 wt.%. The viscosity and density were measured as 3.88 cP and 0.82 g/cc, respectively, at 40°C. The Indiana limestone outcrops with the average block permeability of 135 mD were used for core-flooding experiments. The diameter and the length of the cores were 1.5 and 9 inches, respectively.

B. Transmission Electron Microscopy

A 5 µl volume of solutions of surfactant, PECNP and PECNP-surfactant mixture were placed onto a 300 mesh Lacey carbon copper grid (EMS LC 300 Cu), respectively, for 1 min and blotted twice with a filter paper. The 300-mesh copper grid with PECNP and PECNP-surfactant mixture was examined using a 200 kV FEI Tecnai F20 XT field emission transmission electron microscope at an electron acceleration voltage of 160 kV. TEM images were captured using a normative and standardized electron dose on a eucentric specimen stage and a constant defocus value from the carbon-coated surfaces. Images were randomly acquired in a size of (1024 x1024) pixel resolution at 10 different locations within the grid.

C. Raman Spectroscopy

To perform Raman spectroscopy, solutions of surfactant, PECNP and PECNP-surfactant were freeze dried and Raman spectra of lyophilized powders were obtained by LabRAM ARAMIS Raman spectrometer (LabRAM HORIBA Jobin Yvon, Edison, NJ) equipped with a HeNe laser as an excitation source (λ = 633 nm, power = 17 mW). The instrument specification includes 200 µm confocal hole, 150 µm wide entrance slit, 600 g/mm grating, and 50X long working distance objective Olympus lens. Data acquisition was performed using dedicated software (LabSPEC 5-HORIBA Jobin Yvon). The samples were mounted in a computer-controlled stage and spectra were acquired over a range of 700-2400 cm^{-1} with minimum 60s exposure time and 10-time accumulation. The surfactant spectra was acquired for 1 wt. % concentration in 33,667 ppm salinity brine, since lower concentrations were not resolved with the Raman instrument. The raw data were smoothened and fluorescence backgrounds were removed by subtracting a fifth order polynomial fit to the original spectrum, and contributions of cosmic rays to each spectra were manually removed. The spectra of the mixtures of PECNP and surfactant were fitted with average of surfactant and PECNP spectra using least squares fitting method. Vectors representing each fit were created using the MATLAB's POLYVAL function and residuals were determined.

D. Interfacial Tension and Dilatational Elasticity

The effect of PEI and PECNP on the interfacial properties of $scCO_2$ bubble and dilatational elasticity of the surface was evaluated considering the axisymmetric drop shape analysis of pendant drop in dynamic condition. The chamber in interfacial tension (IFT) setup in Fig. 1 contains the aqueous phase solution and the capillary tip holds the pendant CO_2 bubble in high pressure (1350 psi) chamber filled with Surfactant, PEI or PECNP-surfactant solutions while maintaining isothermal temperature of 40 °C. The bubble photos were taken and analyzed by DROPimage software to calculate the interfacial tension between the $scCO_2$ and different aqueous phases.

The dilatational elasticity was estimated using the ramp-type perturbation approach correlating the relative area compression to surface pressure variation over time [8]. The equilibrium surface dilatational elasticity, E_e, was calculated by measuring the equilibrium portion of the surface pressure change, $\Delta\pi_e$, and calculating $\Delta A/A_i$ ratio using (1).

$$\Delta\pi_e = E_e \Delta A/A_i \quad (1)$$

A_i is the initial surface area prior to mechanical strain. The supplementary information for analysis are found in [4, 8].

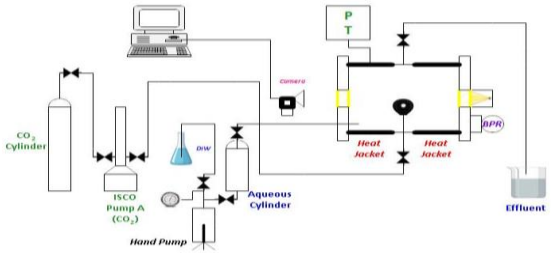

Fig. 1. Schematic of the IFT setup (made by Core Laboratories Inc.), reprinted with permission from [4], Copyright SPE 2018.

E. Core-Flooding by CO_2 Foam

1) $ScCO_2$ foam flooding in the absence of crude oil

Foam flooding experiments were conducted in a multifunctional coreflooding apparatus (Fig. 2) for two different salinities of 33,667 and 67,333 ppm. The PECNPs effect on the foam properties was evaluated by studying the apparent viscosity of different foam systems. The apparent viscosity of foam, μ_{app}, was obtained by applying the steady-state pressure drops along the cores using (2) considering the properties of rocks and fluids [9].

$$\mu_{app} = (kA/q_g + q_l)(|\Delta P|/L) \quad (2)$$

Where q_g and q_l are the flowrates of $scCO_2$ and aqueous phase solution, respectively.

2) $scCO_2$ foamflooding in the presence of crude oil

The process of evaluating the $scCO_2$ foam flooding performance in the presence of crude oil was started with primary drainage under pressure and temperature of 1350 psi and 40°C, respectively. Accordingly, 4 PVs of crude oil was injected into the core with flow rate of 0.5 mL/min until no more water was produced. Monitoring the volume of the injected and collected oil was used to calculate the initial oil saturation, S_o, using (3):

$$S_o = (\text{Inj.oil} - \text{prod. oil})\text{after prim. drain.}/PV \quad (3)$$

The oil production mechanism was started with injecting 4 PVs of brine with flow rate of 0.5 mL/min until no more oil was produced. The recovery efficiency of the water flooding (WF) process, and the residual oil saturation, S_{or}, were calculated using (4) and (5).

$$WF\ \text{eff.}(\%) = \text{Prod. Oil after WF}/OOIP \times 100 \quad (4)$$

$$S_{or} = (S_o PV - \text{Prof. oil due to WF})/PV \quad (5)$$

Thereafter, Surfactant, PEI-surfactant, and PECNP-surfactant generated CO_2 foams were injected through different cores and the recovery efficiency and the residual oil saturation were calculated. The foam quality of 90% and the injection rate of 3 mL/min were used. At the end, cores were flooded with up to 5 PVs of brine.

III. Results and Discussion

A. Transmission Electron Microscopy

Fig 3 represents the TEM images for 0.1 wt.% surfactants, PECNP, and PECNP: surfactant (with 1:9 ratio) prepared in 33,667 ppm salinity brine. The size of nanoparticles and surfactants agree with our previously reported light scattering results [7].

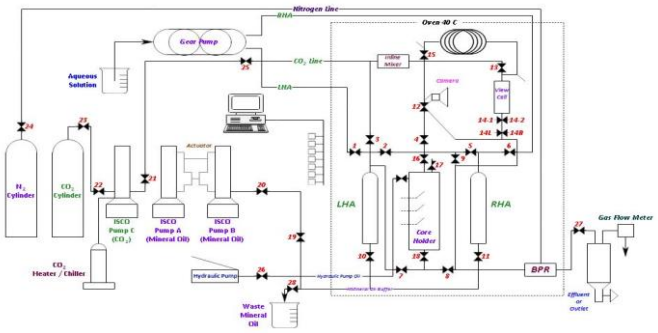

Fig. 2. Schematic of the core flooding system, reprinted with permission from [4], Copyright SPE 2018.

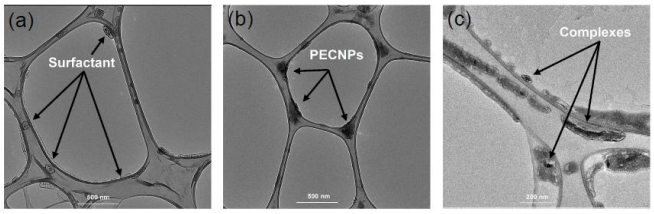

Fig. 3. TEM images for (a) 0.1 wt. % surfactant, (b) PECNP, and (c) complexes of PECNP: Surfactant 1:9 prepared in 33,667 ppm salinity brine

Formation of micellar domains with less than 100 nm dimensions was observed in Fig. 3a for 0.1 wt. % surfactant solution. Electrostatic interactions of PEI and DS polymer chains lead to formation of PECNPs as shown in Fig. 3b. The size range of PECNP domain is ~ 200 nm. Fig. 3c exhibits the complexation of PECNP and N-120 micelles. PECNP aggregation with N-120 micelles creates vesicular structures comprising electrostatically merged nanoparticle and surfactant components. Electrostatic attractions between the amine groups in PECNP, hydrated ether and hydroxide groups in N-120 lead to redistribution and direct bonding of micelles on nanoparticles. Electrostatic complexation is responsible for accumulation of elastic and positively charged hydrophilic particles at the plateau border led to stabilization of lamella interface.

B. Raman Spectroscopy

Raman spectra were obtained for lyophilized samples of brine, sulfate, 1 wt. % surfactant, PECNP and PECNP-surfactant prepared in 33,667 ppm salinity brine. One of the most notable characteristic bands was identified as sulfate centered at 1014 cm^{-1}. The relative intensity of sulfate band varies significantly among the spectra of PECNP, surfactant and the mixture of PECNP-surfactant. The band observed at 1014 cm^{-1} in the PECNP-surfactant spectrum is likely due to contributions from both sulfate and aromatic ring vibrations in N-120 surfactants [3]. The PECNP-surfactant spectrum illustrated in Fig. 4 shares the features of both PECNP and surfactant solutions.

Least-square fitting approach was employed to model the variations in Raman scattering for the mixture of PECNP-surfactant solution in 33,667 ppm salinity brine. A two-component model comprised of an average PECNP and average surfactant spectrum was fitted to PECNP-surfactant spectrum (Fig. 4). Within the spectra, a change in the chemical environment of the components can be detected in the regions where the PECNP-surfactant spectrum is not completely explained by the sum of the components and the presence of well-defined peaks in residual is indicative of a change in chemical environment due to reactions between the individual components. In residual shown in Fig. 4, the sulfate band at 1014 cm^{-1} represents a fingerprint residue and band regions between 1060 to 1100 cm^{-1} and 1615 to 1670 cm^{-1} are not explained by fitted least-square model. As mentioned, the sulfate intensification is due to a change in chemical environment of key functional groups [3, 10]. The residual peaks at 1060 to 1100 cm^{-1} and between 1615 and 1670 cm^{-1} are characteristics of aromatic and aliphatic chain vibrational modes.

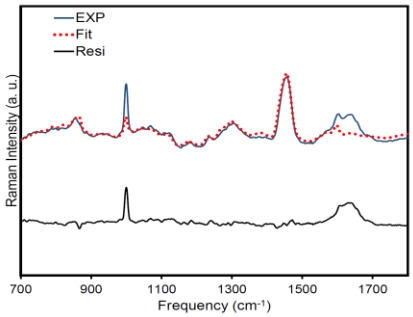

Fig. 4. Raman spectra for PECNP: surfactant (1:9 ratio) (blue line), the fitted curve (red dots) and corresponding residual line (black line).

C. *Interfacial Tension and Dilatational Elasticity*

The relative permeability and capillary pressure of CO_2-brine are critical factors affecting CO_2 displacements for CO_2 storage applications due to the surface tension at the interface of two immiscible fluids [12, 16]. IFT controls the capillary forces along the lamellae, which is a critical property in determining the foam lamellae drainage [11].

Dynamic IFT measurements showed that IFT declines upon addition of PECNP complexes to the surfactant solution [4] and the capillary forces decline. Reorienting the supercharged nanoparticles along the interface improves the DLVO electrostatic repulsions at the interface and stabilizes the lamellae. Hence, foam needs less mechanical energy to move in the small pores. In addition, comparing IFT for two salinities show that IFT is higher for surfactant solution prepared in higher brine concentration. This is due to imbalance forces because of higher presence of ionic interactions. However, addition of supercharged polyelectrolyte complexes to the surfactant solution lowers IFT in higher salinity, which confirms that high electrolyte concentration improves the repulsive forces and it prevents the spontaneous aggregation of nanoparticles [12]. Dilatational elasticity is a measure of the surface tension gradient opposing the film drainage [13] and it is used to evaluate the stability of the thin film liquids with surface pressure variations. Table 1 reveals that addition of PEI and PECNP to the surfactant solution improves the dilatational elasticity significantly. This is due to accumulation of the nanoparticles and forming a viscoelastic layer on the interface [10]. It corresponds to improving the interface elasticity and mechanical strength. The enhanced surface dilatational viscoelasticity maintains bubble with prolonged time and subsequently foam stability is improved [14]. The enhanced foam interfacial layer consisting PECNP-surfactant resists the deformations and shear from geological trappings, paving the way for effective underground CO_2 storage.

Table 1. Equilibrium elasticity of different systems in two salinities.

Aqueous Phase	Equilibrium Elasticity
0.1 wt. % surfactant in MLP 33,667 ppm	3.82
PEI-surfactant in MLP 33,667 ppm	7.94
PECNP-surfactant in MLP 33,667 ppm	9.19
0.1 wt. % surfactant in MLP 67,333 ppm	2.47
PEI-surfactant in MLP 67,333 ppm	7.10
PECNP-surfactant in MLP 67,333 ppm	13.21

D. *Foam Flooding*

The core-flooding experiments were started with measuring porosity and permeability of the cores used in this study. The measured pore volume (PV), porosity (ϕ), and permeability (k) of different cores in Table 2 shows that the porosity and permeability of different core plugs varies between 17 to 19% and 90 to 190 mD, respectively.

Primary flood was performed with injecting 2 PVs of corresponding aqueous phase solution. Subsequently, cores were flooded with $scCO_2$ foam generated with PECNP and surfactant stabilizing mixtures and the pressure gradient was monitored. The Stabilized pressure gradient values are shown in Table 3. The pressure gradient plots can be found in [4].

Core-flooding experimental results reveal the synergistic effect of nanoparticle and chemical additives on the differential pressure in 33,667 ppm salinity brine (Table 3). Addition of PEI to surfactants solution offers a better performance in higher electrolyte concentration (Table 3), due to electrostatic interaction of PEI with surfactant. However, since no electrostatic complexes are formed, it is not preventing movement of surfactant sterically.

Improvement of apparent viscosity associated to each differential pressure in Table 3 indicates that $scCO_2$ foam fluids, comprising the PEI and PECNP addition to N-120 surfactant in high salinity brine, were promising in increasing the differential pressure across the cores. Electrostatic complexation of ionic ingredients in the bulk fluid gives rise to the viscosity, bulk rheological properties, and stabilizes the foam front for oil recovery [4, 7].

Table 4 illustrates different scenarios of foam injections and oil saturation and recovered oil after each flood. Similar injection scenarios involving different foam systems in 33,667 and 67,333 ppm salinity brines were applied to core #17 and #13. Injecting 2 PVs of surfactant enhanced $scCO_2$ foam subsequent to waterflood (33,667 and 67,333 ppm salinity brines, respectively) resulted in recovering 45.33% and 46.60 % of the residual oil in cores #17 and #13, respectively. The foam injection was maintained until complete oil recovery was achieved. Subsequently, the core was flooded with 2.5 PV of PECNP-surfactant generated $scCO_2$ foam.

Table 2. Summary of the measured pore volume, porosity, and permeability for the Indiana limestone cores used for the Core-Flooding experiments in the presence and absence of MLP crude oil.

Cores used in Core-Flooding experiments without oil.				
Core#	***Liquid phase***	***PV (mL)***	***ϕ (frac.)***	***K (mD)***
1	MLP 33,667 ppm	49.136	0.189	156.5
2		48.389	0.186	185.63
7		44.303	0.17	92.79
4	MLP 67,333 ppm	46.169	0.177	191.61
8		45.785	0.176	77.47
9		47.816	0.183	125.52
Cores used in Core-Flooding experiments with oil.				
17	MLP 33,667 ppm	45.059	0.173	150.32
11		45.098	0.173	195.63
19		44.028	0.174	91.74
13	MLP 67,333 ppm	46.494	0.178	127.02
15		47.059	0.181	170.45
18		47.567	0.183	181.86

Table 3. The apparent viscosity of the $scCO_2$ foam with different aqueous phase solutions prepared in two different brines under 2000 s^{-1} shear rate.

Aqueous Phase	*ΔP (psi)*	*μ_{app} (cP)*
0.1 wt. % surfactant in MLP 33,667 ppm	42 ± 2	3.82
PEI-surfactant in MLP 33,667 ppm	75 ± 2	7.94
PECNP-surfactant in MLP 33,667 ppm	145 ± 1	9.19
0.1 wt. % surfactant in MLP 67,333 ppm	20 ± 2	2.47
PEI-surfactant in MLP 67,333 ppm	135 ± 1	7.1
PECNP-surfactant in MLP 67,333 ppm	152 ± 2	13.21

This resulted in 10.00% and 10.75% of the residual oil in place after surfactant-generated $scCO_2$ foam injection in cores #17 and #13, respectively. Eventually, injection of PEI-surfactant $scCO_2$ foam did not offer a promising oil recovery in 33,667 ppm salinity brine (0.8 %). However, it recovered 4.38% of the residual oil in place in 67,333 ppm salinity brine. Comparing the recovery efficiency for two different salinities confirms the efficiency of foams made with lower concentration of brine to recover more oil. Furthermore, PEI-surfactant generated $scCO_2$ foam demonstrates significant gain in production in the last step of flooding scenario in 2X concentration of sea-water equivalent brine.

A different sequence of injection was tested for core #19 and #18 in two different salinities of 33,667 and 67,333 ppm. The foam injection process was started with PECNP-surfactant generated $scCO_2$ foam flood after water flooding and led to 54.35% and 47.71% recovery of the residual oil in place for cores #19 and #18, respectively. More stable foam leads to up to 22% increase in oil recovery in the first step after waterflood. Subsequently, injecting 2.5 PVs of PEI-surfactant generated CO_2 foam recovered 20.46% and 13.82% of the residual oil in place for cores #19 and #18, respectively. Finally, 2.5 PVs of the surfactant enhanced CO_2 foam recovered 2.34% of the residual oil in place for core #19 and 8.02% of the residual oil in place for core #18.

Eventually, cores #11 and #15 were subjected to the last scenario of injection. PEI-surfactant, PECNP-surfactant, and surfactant generated $scCO_2$ foam were injected through the cores after waterflooding. Injection of the 2.5 PVs of PEI-surfactant generated $scCO_2$ foam led to 32.45% and 39.20% recovery of the residual oil in core #11 and #15, respectively. Subsequently, injection of 2.5 PVs of PECNP-surfactant generated $scCO_2$ foam recovered 8.58% and 10.08% of the residual oil in core #11 and #15, respectively. Finally, 2.5 PVs injection of surfactant generated CO_2 foam through the cores recovered 6.57% and 1.12% of the residual oil in core #11 and core #15, respectively.

It was observed that the second scenario was significantly more successful in improving oil recovery and decreasing residual oil saturation. Formation of supercharged complexes stabilized foam front improved oil recovery. The recovery factor and the residual oil saturation values listed in Table 4 exhibit that the second scenario leads to the highest values of recovery factor for both 33,667 and 67,333 ppm salinities of diluted MLP brine. In general, the first scenario is considered for the oil wells subjected to surfactant foam flooding with their current status being at the residual oil saturation condition.

Table 4. Different scenarios of $scCO_2$ foam injection in 33,667 and 67,333 ppm salinity brines. The percentages are based on the oil in place at the end of the previous flood. The values with a * sign were neglected based on the error limits. Reprinted with permission from [4], Copyright SPE 2018.

First Scenario				
Salinity	***33,667 ppm***	***33,667 ppm***	***67,333 ppm***	***67,333 ppm***
Core Number	***Core#17***	***Core #17***	***Core #13***	***Core #13***
System	***S_o (fraction)***	***Recovered Oil (%)***	***S_o (fraction)***	***Recovered Oil (%)***
Primary Drainage	0.612		0.654	
Water flooding	0.284	53.58	0.35	46.6
Surfactant generated CO_2 foam	0.155	45.33	0.22	36.96
PECNP-surfactant generated CO_2 foam	0.14	10	0.196	10.75
PEI-surfactant generated CO_2 foam	0.139*	0.8	0.188*	4.38
Second Scenario				
Salinity	***33,667 ppm***	***33,667 ppm***	***67,333 ppm***	***67,333 ppm***
Core Number	***Core #19***	***Core #19***	***Core #18***	***Core #18***
System	***S_o (fraction)***	***Recovered Oil (%)***	***S_o (fraction)***	***Recovered Oil (%)***
Primary Drainage	0.512		0.54	
Water flooding	0.267	47.76	0.291	46.17
PECNP-surfactant generated CO_2 foam	0.122	54.35	0.152	47.71
PEI-surfactant generated CO_2 foam	0.097	20.46	0.131	13.82
Surfactant generated CO_2 foam	0.095*	2.34	0.123*	8.02
Third Scenario				
Salinity	***33,667 ppm***	***33,667 ppm***	***67,333 ppm***	***67,333 ppm***
Core Number	***Core #11***	***Core #11***	***Core #15***	***Core #15***
System	***S_o (fraction)***	***Recovered Oil (%)***	***S_o (fraction)***	***Recovered Oil (%)***
Primary Drainage	0.715		0.648	
Water flooding	0.383	46.45	0.35	45.93
PECNP-surfactant generated CO_2 foam	0.259	32.45	0.213	39.2
PECNP-surfactant generated CO_2 foam	0.236	8.58	0.192	10.08
Surfactant generated CO_2 foam	0.221*	6.57	0.190*	1.12

Injection of the PECNP-surfactant generated $scCO_2$ foam after surfactant foam flooding recovered 10% of the residual oil in place due to improved stability of the PCNP-generated $scCO_2$ foams in the presence of crude oil. Electrostatic hindrance of the polyelectrolyte complex nanoparticles to the N-120 surfactants stabilizes the interface by preventing the surfactants from leaving the interface and leading to formation of a very stable foam front in the presence of crude oil in high salinity environments. PEI adds to charge density and stability of the interface as well. However, PEI charge density and colloidal stability is not sufficient to compete with repulsion forces offered by PECNP-surfactant complexes.

IV. Conclusions

Herein, we reported the improved capability of dry $scCO_2$ foams stabilized with PECNP for EOR applications, CO_2 storage and sequestration. The high internal phase emulsion stabilized with PECNP combines the improved viscosity and stability to flow in geological formations and improve sweep efficiency. A novel mixture containing surfactant and PECNP is effective in immobilization of lamella, rigidity improvement and electrostatic repulsion in CO_2-water interface to improve the recovery while the gas phase is stored partially. The major conclusions are summarized as following:

1. The presented mixture offers the potential to reduce produced water disposal and fresh water usage for EOR. The chemical compatibility with produced water introduces a viable solution for sustainability of water-based energy production and environmentally friendly approach to manage the water resources.

2. TEM imaging and Raman spectroscopy analysis confirm the electrosteric interaction of PECNP with surfactant micelles as wormlike or vesicular structures comprising both nanoparticle and surfactant components. The ionic nano-structures offer IFT reduction and improve the lamellae rigidity, opposing the lamella drainage and bubble coalescence. Raman spectroscopy results identified three major spectral regions not explained by the surfactant and PECNP spectra alone, indicating a change in chemical environment of the key functional groups due to ionic complexation and reorganization of the aromatic and aliphatic chain components.

3. The developed system is capable of enhancing interfacial interactions and disjoining pressure of the foam film and provides improved DLVO forces in aqueous polyelectrolytes for carbonate surfaces. The results demonstrate the superior capability of PECNP-surfactant conjugation in homogenous microcellular foam formation with lowering IFT and improving the dilatational elasticity and mechanical strength at the interface. Due to chemical compatibility of the mixture with high electrolyte concentration, PECNP-surfactant mixtures represent a new prospect for stabilizing the thin films in a high salinity environment.

4. Addition of PECNP to surfactant solution improved the sweep efficiency and oil recovery from carbonate reservoirs employing high concentration of brine electrolytes. The highest-pressure drop and correspondingly the highest average effective viscosity were observed for PECNP-surfactant generated $scCO_2$ foam. Several scenarios of foam injection indicated the highest incremental oil recovery and the lowest oil saturation were achieved by prioritizing PECNP-surfactant $scCO_2$ foam flood in both electrolyte concentrations. Furthermore, injecting the PECNP- surfactant generated $scCO_2$ foam into the cores that were in residual oil saturation state recovered 10% of the residual oil in place.

Acknowledgements

Authors would like to thank the National Science Foundation EPSCoR Research Infrastructure Improvement Program: Track-2 Focused EPSCoR Collaboration award (OIA-1632892) and the Kansas Interdisciplinary Carbonates Consortium (KICC) for funding the project. We would also like to thank Dr. Cory J, Berkland, Dr. Prem S. Thapa, Stephanie Johnson, Zach Kessler, and Scott Ramskill, at the University of Kansas for their help and supports.

V. References

[1] L. Jiang, M. Yu, Y. Liu, M. Yang, Y. Zhang, Z. Xue, T. Suekane and Y. Song, "Behavior of CO2/water flow in porous media for CO_2 geological storage," Magn Reson Imaging, vol. 37, pp. 100-106, 2017.

[2] G. G. Bernard and L. W. Holm, "Method for Recovering Oil from Subterranean Formations". United States Patent US 3342256, 19 9 1967.

[3] H. Hosseini, J. S. Tsau, K. Shafer-peltier, C. Marshall, Q. Ye and R. B. Ghahfarokhi, "Experimental and Mechanistic Study of Stabilized Dry CO_2 Foam Using Polyelectrolyte Complex Nanoparticles Compatible with Produced Water To Improve Hydraulic Fracturing Performance," Ind. Eng. Chem. Res., vol. 58, no. 22, pp. 9431-9449, 2019.

[4] N. Nazari, J. Tsau and R. Barati, "Improving CO_2 Foam for EOR Applications Using Polyelectrolyte Complex Nanoparticles Tolerant of High Salinity Produced Water," in SPE Improved Oil Recovery Conference, Tulsa, Oklahoma, USA, 2018.

[5] C. Patel, M. A. Barrufet and A. B. Petriciolet, "Effective Resource Management of Produced Water in Oil and Gas Operations," in Canadian International Petroleum Conference, Alberta, Canada, 2004.

[6] N. Kristen and R. V. Klitzing, "Effect of Polyelectrolyte/Surfactant Combinations on the Stability of Foam Films," Soft Matter, vol. 6, no. 5, pp. 849-861, 2010.

[7] N. Nazari, J. S. Tsau and R. Barati, "CO_2 Foam Stability Improvement Using Polyelectrolyte Complex Nanoparticles in Produced Water," Journal of Energies, vol. 10, no. 4, 2017.

[8] F. Tewes, M. P. Krafft and F. Boury, "Dynamical and Rheological Properties of Fluorinated Surfactant Films Adsorbed at the Pressurized CO_2–H_2O Interface," Langmuir, vol. 27, no. 13, p. 8144–8152, 2011.

[9] S. Kahrobaei, S. Vincent-Bonnieu and R. Farajzadeh, "Experimental Study of Hysteresis Behavior of Foam Generation in Porous Media," Scientific Reports, vol. 7, pp. 1-9, 2017.

[10] N. Nazari, H. Hosseini, J. S. Tsau, K. Shafer-Peltier, C. P. Marshall and R. Barati, "Development of Highly Stable Lamella Using Polyelectrolyte Complex Nanoparticles: An Environmentally Friendly scCO2 Foam Injection Method for Greenhouse Gas Management," MIT Applied Energy A+B Conference, Boston, MA, USA, 2019.

[11] C. J. W. Breward and P. D. Howell, "The Drainage of a Foam Lamella," Journal of Fluid Mechanics, vol. 458, pp. 379-406, 2002.

[12] B. Behdani, S. Monjezi, M. J. Carey, C. G. Weldon, J. Zhang, C. Wang and J. Park, "Shape-Based Separation of Micro-/ Nanoparticles in Liquid Phases. 2018;12:2-26.," AIP Biomicrofluidics, vol. 12, no. 5, 2018.

[13] L. L. Schramm, Foam, Fundamentals and Applications in Petroleum Industry, Washington D.C., USA: Americal Chemical Society, 1994.

[14] Q. Sun, Z. Li, S. Li, L. Jiang, J. Wang and P. Wang, "Utilization of Surfactant-Stabilized Foam for Enhanced Oil Recovery by Adding Nanoparticles," Energy and Fuels, vol. 28, no. 4, p. 2384–2394, 2014.